Efficiency Improvement of Permanent Magnet BLDC Motors for Electric Vehicles

Dinh Bui Minh
School of Electrical Engineering
Hanoi University of Science and Technology
Vietnam
dinh.buiminh@hust.edu.vn

Vuong Dang Quoc
School of Electrical Engineering
Hanoi University of Science and Technology
Vietnam
vuong.dangquoc@hust.edu.vn

Phuong Nguyen Huy
School of Electrical Engineering
Hanoi University of Science and Technology
Vietnam
phuong.nguyenhuy@hust.edu.vn

Abstract-A permanent magnet Brushless DC (BLDC) motor has been designed with different rotor configurations based on the arrangement of the permanent magnets. Rotor configurations strongly affect the torque and efficiency performance of permanent magnet electric motors. In this paper, different rotor configurations of the permanent magnet BLDC motor with parallel the Halbach array permanent magnet were compared and evaluated. Many applications of electric drives or air-crafts have recently preferred the surface-mounted permanent magnet design due to its ease of construction and maintenance. The finite element technique has been used for the analysis and comparison of different geometry parameters and rotor magnet configurations to improve efficiency and torque performance. A comprehensive design of a three-phase permanent magnet BLDC 35kW motor is presented and simulations were conducted to evaluate its design. The skewing rotor and Halbach magnet array are applied to the permanent surface-mounted magnet on the BLDC motor for eliminating torque ripples. In order to observe the skewing rotor effect, the rotor lamination layers were skewed with different angles and Halbach sinusoidal arrays. The determined skewing angle, the eliminated theoretically cogging torque, and the back electromotive force harmonics were also analyzed.

Keywords-BLDC; permanent magnet; finite element method; Ansys Maxwell; SPEED; magnetic flux density

I. INTRODUCTION

Permanent magnet (PM) Brushless DC (BLDC) motors are widely used due to features such as compactness, low weight, high efficiency, and easy assembly [1, 2]. The reliability of BLDC motor is high since it is easy to mount the PM and has a robust structure. Different rotor configurations are available for the PM BLDC motor, e.g. the surface mounted PM design with the interior/exterior rotor, the interior PM design with buried magnets due to specific strengths and weaknesses [3-5]. Among these, there are the radial-flux motors, the surface mounted types with different magnet arrangement that have been used for electrical drives. This paper introduces a novel design of the BLDC35kW-Z36P12 rotor with high efficiency and low torque ripple. The electromagnetic performance of the PM BLDC with 36 stator slots and 12 rotor poles is discussed in this paper.

Corresponding author: Vuong Dang Quoc

II. ELECTROMAGNETIC TORQUE ANALYSIS

The aim is to lower the cost with high overload efficiency and reliability. High efficiency and torque density for electric vehicle applications are the first priorities of this design program. The calculation process of the proposed BLDC motor conducted with the SPEED software is presented in Figure 1. The geometry specifications of the motor used for the analysis are given in Table I.

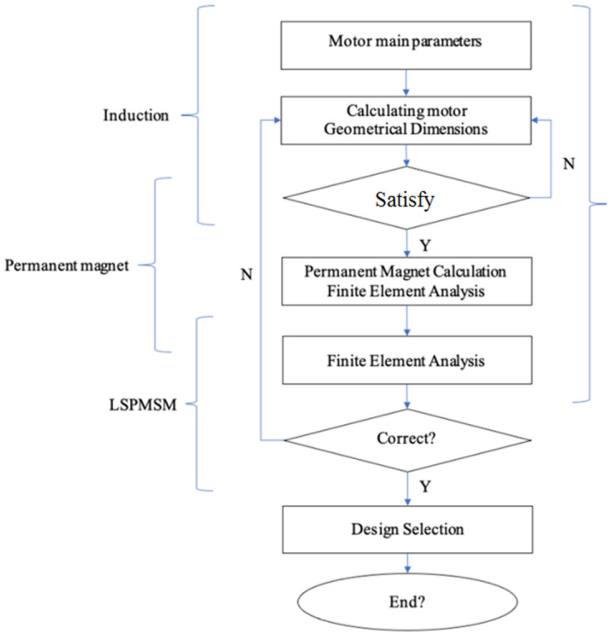

Fig. 1. Design calculation process.

TABLE I. GEOMETRY SPECIFICATIONS OF THE PM BLDC MOTOR

No	Parameters	Unit
1	Outer diameter	218 mm
2	Rotor diameter	142 mm
3	Slot length	112 mm
4	Normal torque	200 Nm
5	Maximum torque	350 Nm
6	Speed	3600 rpm

The geometry dimensions of the PM BLDC motor are saved in a database in matrix form. When the export command is generated, the drawing process will be executed. The program is developed with the MATLAB DXF library shown in Figure 2. For the drawing circle line, rotating object of stator slots, 2D modeling is implemented to get geometrical formulas of the circle lines. The algorithm needs to satisfy two requirements: the shape of these lines must be similar to the desired curves and the least possible points must be used. Using the minimum number of lines will help the system because it will not have to store a lot of data, which will slow down speed and present difficulties at exporting the drawings. On the other hand, rotation and mirroring are difficult tasks in programming. The strategy is to use a loop function to redraw several times and trigonometric function with angle steps was applied returning good results.

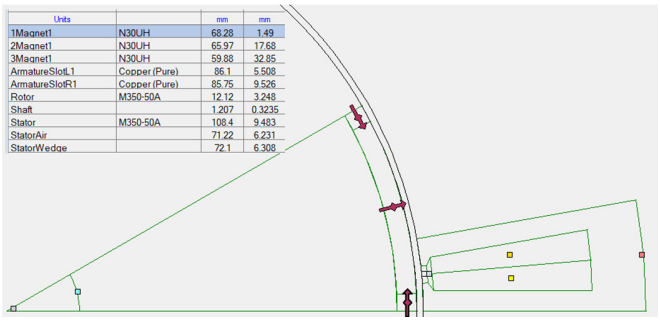

Fig. 2. MATLAB DXF drawing.

The system will export separate drawings of the motor, the rotor, and the stator. These drawings can be used in several simulation programs and in the design and manufacturing progress. The detail parameters are shown in Table II.

TABLE II. DESIGN PARAMETERS OF PM BLDC MOTOR

Parameters	Values	Unit
Stator bore	142	mm
Tooth width	7	mm
Slot depth	29	mm
Tooth tip depth	1	
Slot opening	3	
Tooth tip angle	30	degrees
Pole number	12	
Magnet thickness	4	mm
Housing dia	228	mm
Stator lam dia	218	mm
Stator bore	142	mm
Airgap	1	mm

Programs can support the material weight and volume calculation because the power and torque density are also important factors in each motor design. From the geometry parameters, the material weights of two PM BLDC motors were obtained and are shown in Table III. The two PM BLDC motors with the parallel magnet and the Halbach magnet array are presented in Figure 3. The magnet thickness of the conventional design is 4 mm and the electric angle is 150^0 while the Halbach magnet array has a thickness of 3.5 mm and 175 electric embraces. The total weight of a novel design of the Halbach magnet is lower with the same magnet weight.

TABLE III. WEIGHT DETAILS OF THE PM BLDC MOTORS

Parameters	Material	Parallel	Halbach
Stator lam (back iron)	M350-50A	3.947	3.947
S tator lam (yooth)	M350-50A	4.967	4.317
Stator lamination [total]		8.913	8.263
Armature winding [active]	Copper (Pure)	3.23	3.621
Armature EWdg [front]	Copper (Pure)	1.273	0.4767
Armature EWdg [rear]	Copper (Pure)	1.273	0.4767
Armature winding [total]		5.777	4.575
Rotor lam (back iron)	M350-50A	8.811	8.811
Rot inter lam (back iron)		4.02E-05	4.02E-05
Rotor lamination [total]		8.812	8.812
Magnet	N30UH	0.9613	0.9613
Total		25.42	23.57

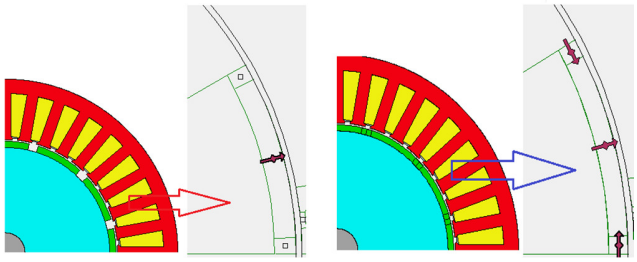

Fig. 3. BLDC motor p=12, Z=36 parrallel magnet (left) and Halbach magnet (right).

Electro Magnetic Force (EMF) and torque, calculated by a MATLAB analytical coupling program with the Finite Element Method (FEM) are expressed as [11, 12]:

$$\Phi_g = B_g \times \frac{\pi D L_{stk}}{p} \quad (1)$$

$$E_a = \frac{2p}{\pi} w_m T_{ph} \Phi_g \quad (2)$$

$$T_e = \frac{\sqrt{3}}{2} p k_w T_{ph} \Phi_g i_{Lpk} \quad (3)$$

where T_{ph} is the turn per phase term, T_e is the electromagnetic torque and E_a is the back EMF.

The electromagnetic performances based on this design are shown in Table IV. The most important parameter is the efficiency of 93.792%. The efficiency of Halbach magnet and skewed rotor with 5 slices is optimized by the control current of 250A with 200VDC.

TABLE IV. ELECTROMAGNETIC PERFORMANCE COMPARISON

Parameters	Parallel Magnet	Halbach Magnet	Unit
Average torque	226.42	243.41	Nm
Torque ripple	24.635	13.081	Nm
Torque ripple [%]	10.815	5.3608	%
Cogging torque ripple	20.709	4.4287	Nm
Input power	38555	96326	W
Output power	35389	90347	W
Total losses	3165.9	5979.7	W
System efficiency	91.789	93.792	%
Shaft torque	225.3	239.65	Nm

In order to evaluate the maximum torque of the motor, a maximum current is applied to determine when the permanent magnetic is irrecoverable. The maximum torque is 350 Nm at the speed of 1500 rpm with a current of 500 A. Efficiency is calculated based on copper and iron losses. Those losses depend on the stator and rotor teeth dimensions. An efficiency map of the Halbach magnet array with rotor skewed slices is shown in Figure 4.

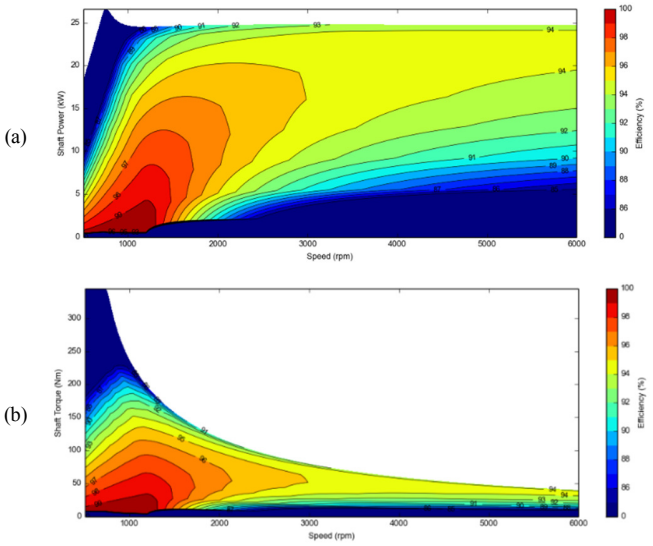

Fig. 4. Efficiency map of (a) Power and (b) Torque.

The torque and speed operation areas have been plotted with different efficiency values. The maximum torque acquired is 350 Nm at the speed of 1000 rpm with low efficiency of 79%. A 2D BLDC motor model is solved and simulated by FEM [13-15]. After meshing the geometry model including the magnetic, the silicon steel, and the insolation materials, the flux density distribution of rotor and stator, is shown in Figure 5.

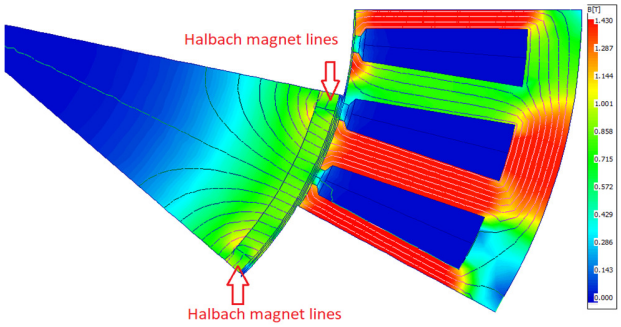

Fig. 5. Flux density results.

The flux density of the air gaps is investigated in one pole. Many steps of rotor position, currents, torque, and flux density were recorded and saved in Matlab files to plot those characteristics. The leakage flux lines are enclosed to air gap areas, which also helps to increase the flux density and reduce the rotor yoke iron loss.

III. TORQUE RIPPLE ANALYSIS OF ROTOR SKEWED SLICES

Skewing slices of rotor are frequently used in PM BLDC motors for eliminating the cogging torque. For the optimum skew angle of those slices, the cogging torque can be eliminated theoretically. The skewed slots for the rotor slices are illustrated in Figure 6.

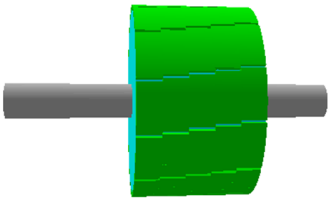

Slice	Proportional	Angle
		Mech Deg
Slice 1	1	-4
Slice 2	1	-2
Slice 3	1	0
Slice 4	1	2
Slice 5	1	4

Fig. 6. Rotor skewing slices.

The torque ripple results are shown in Figure 7. The cogging torque can be calculated by the stored energy in the air gap. The variation of the co-energy given the cogging torque is expressed as [6-8]:

$$T_c = \frac{dW}{d\theta} \quad (4)$$

where T_c is the cogging torque, $\partial\theta$ is the displacement with mechanical degree, and ∂W is the stored co-energy in the air gap.

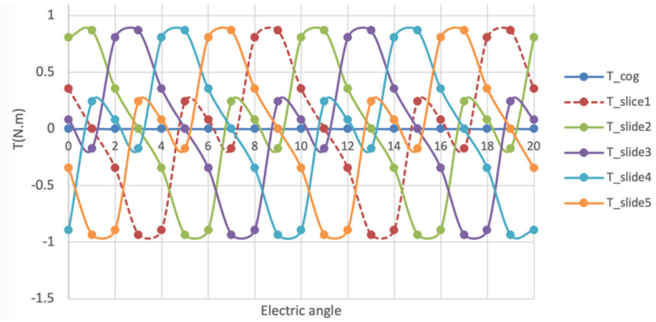

Fig. 7. Torque ripple analysis.

The cogging torque is periodic along the air gap. By using this periodicity feature, the Fourier series of the cogging torque can be obtained [6, 7]:

$$T_{skew}(\theta) = \sum_{i=1}^{\infty} K_{sk} \cdot T_i \cdot \sin(iC_p\theta_m + \theta_i) \quad (5)$$

where K_{sk} is the skew factor that is 1 for non-skewed motor laminations, C_p is the least common multiple of the number of poles and number of stator slots, T_i is the absolute value of the harmonic i, θ_m is the mechanical angle between the stator and the rotor axis while the motor is rotating, and θ_i represents the phase angle. The skew factor K_{sk} is defined by:

$$K_{sk} = \frac{Sin(\frac{iC\pi\alpha_{sk}}{N_s})}{iC\pi\alpha_{sk}/N_s} \quad (6)$$

where α_{sk} is the skew angle and N_s is the number of the slide. The average values of load torques are nearly the same values for even one slot pitch skewed motor result in terms of average

load torque that are coherent with the non-skewed motor model. The relative torque ripples can be defined as:

$$T_{ripple} = \frac{(T_{max} - T_{min})}{T_{avg}} \quad (7)$$

If the skew angle is increased, the torque ripple is reduced along with the average torque, so for optimal torque performance the ratio of magnetic pole/stator slots needs to be increased.

IV. CONCLUSION

In this paper, a comprehensive design of the PM BLDC motor for electric vehicles has been presented. The design was computed by the analytical method, it was optimized by the SPEED software and the electromagnetic characteristics were evaluated by FEM. In particular, the parallel and Halbach PM array rotor with skewed slides have been compared in terms of efficiency, torque, and cogging torque. The torque ripple is minimum with a skew angle of 8 degrees. The best skewing angle is determined by a stator slot angle of 10 degrees. For the electrical drive, the PM surface mounted motor is easy to arrange Halbach and skewing structures.

ACKNOWLEDGEMENT

The authors wish to thank the Technical University of Berlin for providing the means and conditions needed to carry out this work.

REFERENCES

[1] Y. Park, H. Kim, H. Jang, S.-H. Ham, J. Lee, and D.-H. Jung, "Efficiency Improvement of Permanent Magnet BLDC With Halbach Magnet Array for Drone," *IEEE Transactions on Applied Superconductivity*, vol. 30, no. 4, pp. 1–5, Jun. 2020, https://doi.org/10.1109/TASC.2020.2971672.

[2] P. Ji, W. Song, and Y. Yang, "Overview on application of permanent magnet brushless DC motor," *Electrical Machinery Technology*, vol. 40, pp. 32–36, 2003.

[3] B. V. R. Kumar and K. S. Kumar, "Design of a new Dual Rotor Radial Flux BLDC motor with Halbach array magnets for an electric vehicle," in *2016 IEEE International Conference on Power Electronics, Drives and Energy Systems (PEDES)*, Trivandrum, India, Dec. 2016, https://doi.org/10.1109/PEDES.2016.7914552.

[4] A. Vadde and S. Sachin, "Influence of Rotor Design in BLDC Motor for Two -Wheeler Electric Vehicle," in *2021 1st International Conference on Power Electronics and Energy (ICPEE)*, Bhubaneswar, India, Jan. 2021, https://doi.org/10.1109/ICPEE50452.2021.9358520.

[5] V. R. Bommadevara, "Design of a High Power density Halbach BLDC Motor for Electric Vehicle Propulsion.," in *2018 IEEE International Magnetics Conference (INTERMAG)*, Singapore, Apr. 2018, https://doi.org/10.1109/INTMAG.2018.8508741.

[6] L. Dosiek and P. Pillay, "Cogging Torque Reduction in Permanent Magnet Machines," *IEEE Transactions on Industry Applications*, vol. 43, no. 6, pp. 1565–1571, Nov. 2007, https://doi.org/10.1109/TIA.2007.908160.

[7] R. Krishnan, *Switched Reluctance Motor Drives: Modeling, Simulation, Analysis, Design, and Applications*, 1st ed. Boca Raton, FL, USA: CRC Press, 2001.

[8] V. D. Quoc, "Robust Correction Procedure for Accurate Thin Shell Models via a Perturbation Technique," *Engineering, Technology & Applied Science Research*, vol. 10, no. 3, pp. 5832–5836, Jun. 2020, https://doi.org/10.48084/etasr.3615.

[9] V. D. Quoc, "Accurate Magnetic Shell Approximations with Magnetostatic Finite Element Formulations by a Subdomain Approach," *Engineering, Technology & Applied Science Research*, vol. 10, no. 4, pp. 5953–5957, Aug. 2020, https://doi.org/10.48084/etasr.3678.

[10] R. Islam, I. Husain, A. Fardoun, and K. McLaughlin, "Permanent-Magnet Synchronous Motor Magnet Designs With Skewing for Torque Ripple and Cogging Torque Reduction," *IEEE Transactions on Industry Applications*, vol. 45, no. 1, pp. 152–160, Jan. 2009, https://doi.org/10.1109/TIA.2008.2009653.

[11] M. D. Bui, S. Schneider, S. Arnaout, and U. Schaefer, "Torque maximization of a high-speed switched reluctance starter in acceleration test," in *2013 15th European Conference on Power Electronics and Applications (EPE)*, Lille, France, Sep. 2013, https://doi.org/10.1109/EPE.2013.6631908.

[12] D. B. Minh, L. D. Hai, T. L. Anh, and V. D. Quoc, "Electromagnetic Torque Analysis of SRM 12/8 by Rotor/Stator Pole Angle," *Engineering, Technology & Applied Science Research*, vol. 11, no. 3, pp. 7187–7190, Jun. 2021, https://doi.org/10.48084/etasr.4168.

[13] M. Yildirim and H. Kurum, "Influence of Poles Embrace on In-Wheel Switched Reluctance Motor Design," in *2018 IEEE 18th International Power Electronics and Motion Control Conference (PEMC)*, Budapest, Hungary, Aug. 2018, pp. 562–567, https://doi.org/10.1109/EPEPEMC.2018.8521859.

[14] A. Tap, L. Xheladini, T. Asan, M. Imeryuz, M. Yilmaz, and L. T. Ergene, "Effects of the rotor design parameters on the torque production of a PMaSynRM for washing machine applications," in *2017 International Conference on Optimization of Electrical and Electronic Equipment (OPTIM) 2017 Intl Aegean Conference on Electrical Machines and Power Electronics (ACEMP)*, Brasov, Romania, May 2017, pp. 370–375, https://doi.org/10.1109/OPTIM.2017.7974998.

[15] V. Q. Dang and C. Geuzaine, "Two-way coupling of thin shell finite element magnetic models via an iterative subproblem method," *COMPEL - The international journal for computation and mathematics in electrical and electronic engineering*, vol. 39, no. 5, pp. 1085–1097, Jan. 2020, https://doi.org/10.1108/COMPEL-01-2020-0035.